DOI: 10.1021/ic900756u

Inorganic Chemistry
Article

Explorations of New Phases in the Ga^{III}/In^{III}-Cu^{II}-Se^{IV}-O System

Fang Kong,[†,‡] Qi-Pu Lin,[†,‡] Fei-Yan Yi,[†,‡] and Jiang-Gao Mao*[,†]

[†]*State Key Laboratory of Structural Chemistry, Fujian Institute of Research on the Structure of Matter, Chinese Academy of Sciences, Fuzhou 350002, People's Republic of China, and* [‡]*Graduate School of the Chinese Academy of Sciences, Beijing, 100039, People's Republic of China*

Received April 20, 2009

Four new gallium(III)/indium(III), copper(II), selenium(IV) oxides, namely, $Ga_2Cu(SeO_3)_4$ (**1**), $Ga_2CuO(SeO_3)_3$ (**2**), and $M_2Cu_3(SeO_3)_6$ (M = Ga **3**, In **4**), have been synthesized by hydrothermal or high-temperature solid-state reactions. The structure of $Ga_2Cu(SeO_3)_4$ (**1**) features a 2D layer of corner-sharing GaO_6 and CuO_6 octahedra with the SeO_3 groups hanging on both sides of the 2D layer. $Ga_2CuO(SeO_3)_3$ (**2**) features a pillared layered structure in which the 1D $Cu(SeO_3)_3^{4-}$ chains act as the pillars between 2D layers formed by corner- and edge-sharing GaO_n (n = 4, 5) polyhedra. Although the chemical compositions of $M_2Cu_3(SeO_3)_6$ (M = Ga **3**, In **4**) are comparable, they belong to two different structural types. $Ga_2Cu_3(SeO_3)_6$ (**3**) exhibits a pillared layered structure built by $[Ga_2Cu_3(SeO_3)_4]^{4+}$ thick layers with $Se(3)O_3^{2-}$ groups as pillars. The structure of $In_2Cu_3(SeO_3)_6$ (**4**) features a 3D network composed of $[In_2(SeO_3)_2]^{2+}$ layers and $[Cu_3(SeO_3)_4]^{2-}$ layers interconnected through Se−O−Cu and In−O−Cu bridges, exhibiting 8-MR helical tunnels along the *a*-axis. Results of magnetic property measurements indicate that there are considerable antiferromagnetic interactions between copper(II) centers in $Ga_2CuO(SeO_3)_3$ (**2**) and $M_2Cu_3(SeO_3)_6$ (M = Ga **3**, In **4**). Interestingly, $Ga_2Cu_3(SeO_3)_6$ (**3**) behaves as a weak ferromagnet below the critical temperature of T_c=15 K. Further magnetic studies indicate that the compound is a canted antiferromagnet with a large canting angle of about 7.1°.

Introduction

Studies concerning metal selenites and tellurites are of great interest to scientists in chemistry and materials due to the presence of the lone pairs of Se(IV) and Te(IV) cations, which are subject to second-order Jahn−Teller (SOJT) distortions and aid in the formation of noncentrosymmetric structures (NCS) with possible second-harmonic generation (SHG).[1−5] Transition metal ions with d^0 electronic configurations such as W^{6+} and Mo^{6+}, which are also susceptible to SOJT distortions, have been successfully introduced to the metal selenite or tellurite systems to enhance their SHG properties.[2−4] Furthermore, in transition metal−selenite or tellurite halide compounds, the lone-pair cations are found to form bonds with only oxygen atoms, whereas the transition metal ion can form bonds with both oxygen and halide anions. Hence, transition metal Te(IV) or Se(IV) oxyhalides can be regarded as "chemical scissors" and are able to form low-dimensional structures. A few promising new low-dimensional magnets have been obtained,[6,7] including $Cu_2Te_2O_5X_2$ (X = Cl, Br), $Cu_3(TeO_3)_2Br_2$, $Cu_3(SeO_3)_2Cl_2$, and $Cu_9O_2(SeO_3)_4Cl_6$.[6b,8] Studies from our group indicate that the activation of the selenite or tellurite anion for the lanthanide(III) ions can produce new luminescent materials in the UV, visible, or near-IR region.[9] As for the post transition metal main group selenites or tellurites, the group 13 compounds have attracted much research attention due to

*To whom correspondence should be addressed. Fax: (+86)591-83714946. E-mail: mjg@fjirsm.ac.cn.

(1) (a) Wickleder, M. S. *Chem. Rev.* **2002**, *102*, 2011 (and references therein). (b) Verma, V. P. *Thermochim. Acta* **1999**, *327*, 63 (and references therein). (c) Ok, K. M.; Halasyamani, P. S. *Chem. Soc. Rev.* **2006**, *35*, 710.
(2) (a) Ra, H.-S.; Ok, K.-M.; Halasyamani, P. S. *J. Am. Chem. Soc.* **2003**, *125*, 7764. (b) Ok, K.-M.; Halasyamani, P. S. *Inorg. Chem.* **2004**, *43*, 4248.
(3) (a) Hart, R. T.; Ok, K.-M.; Halasyamani, P. S.; Zwanziger, J. W. *Appl. Phys. Lett.* **2004**, *85*, 938. (b) Goodey, J.; Broussard, J.; Halasyamani, P. S. *Chem. Mater.* **2002**, *14*, 3174.
(4) (a) Johnston, M. G.; Harrison, W. T. A. *Inorg. Chem.* **2001**, *40*, 6518. (b) Balraj, V.; Vidyasagar, K. *Inorg. Chem.* **1999**, *38*, 5809.
(5) (a) Kong, F.; Huang, S.-P.; Sun, Z.-M.; Mao, J.-G.; Cheng, W.-D. *J. Am. Chem. Soc.* **2006**, *128*, 7750. (b) Mao, J.-G.; Jiang, H.-L.; Kong, F. *Inorg. Chem.* **2008**, *47*, 8498.
(6) (a) Becker, R.; Johnsson, M.; Kremer, R.; Lemmens, P. *Solid State Sci.* **2003**, *5*, 1411. (b) Johnsson, M.; Törnroos, K.-W.; Mila, F.; Millet, P. *Chem. Mater.* **2000**, *12*, 2853.
(7) (a) Millet, P.; Bastide, B.; Pashchenko, V.; Gnatchenko, S.; Gapon, V.; Ksari, Y.; Stepanov, A. *J. Mater. Chem.* **2001**, *11*, 1152. (b) Johnsson, M.; Törnroos, K.-W.; Lemmens, P.; Millet, P. *Chem. Mater.* **2003**, *15*, 68.
(8) (a) Effenberger, H. *Z. Kristallogr.* **1986**, *175*, 61. (b) Kohn, K.; Inoue, K.; Horie, O.; Akimoto, S. *J. Solid State Chem.* **1976**, *18*, 27. (c) Meunier, G.; Svensson, C.; Carpy, A. *Acta Crystallogr. B* **1976**, *32*, 2664.
(9) (a) Shen, Y.-L.; Jiang, H.-L.; Xu, J.; Mao, J.-G.; Cheah, K.-W. *Inorg. Chem.* **2005**, *44*, 9314. (b) Jiang, H.-L.; Ma, E.; Mao, J.-G. *Inorg. Chem.* **2007**, *46*, 7012.

Published on Web 06/18/2009

their good ion exchange or SHG properties.[10−13] It is well known that gallium(III) or indium(III) can exhibit various coordination geometries (MO_4 tetrahedron, MO_5 square-pyramid, or MO_6 octahedron), which offer great opportunities to design new materials with novel topologies and interesting physical properties. So far reports on quaternary Ga(III)/In(III) selenites or tellurites are still scarce except for a few phases in the alkali metals−Ga(III)/In(III)−Se(IV)/Te(IV)−O system.[10−13] We deem that the introduction of a Cu(II) ion into the gallium(III) or indium(III) selenites may lead to quaternary phases with novel structures and interesting magnetic properties. So far, no such compounds have been reported. Our efforts on this aspect afforded four new gallium(III)/indium(III), copper(II) mixed metal selenites, namely, $Ga_2Cu(SeO_3)_4$ (**1**), $Ga_2CuO(SeO_3)_3$ (**2**), and $M_2Cu_3(SeO_3)_6$ (M = Ga **3**, In **4**). Herein, we report their syntheses, crystal structures, and magnetic properties.

Experimental Section

Materials and Instrumention. All reagents were obtained from commercial sources and used without further purification. Powder X-ray diffraction (PXRD) patterns (Cu Kα) were collected on an XPERT-MPD $\theta-2\theta$ diffractometer. The simulated PXRD patterns were calculated using single-crystal X-ray diffraction data and processed by the free Mercury V1.4 program provided by the Cambridge Crystallographic Data Centre. Variable-temperature (2.0−300 K) magnetic susceptibility measurements on polycrystalline samples were carried out with a Quantum Design PPMS model 6000 magnetometer operating at different magnetic fields. Magnetization and hysteresis studies were carried out at 2.0 K in the field range of 0−8 T. Alternating current susceptibility measurements were performed in the frequency range of 311−1311 Hz and under an oscillating magnetic field of 3 Oe. The experimental susceptibilities were corrected for the diamagnetism by using Pascal's constants. Thermogravimetric analyses (TGA) were carried out with a NETZSCH STA 449C unit, at a heating rate of 10 °C/min under an air atmosphere. IR spectra were recorded on a Magna 750 FT-IR spectrometer photometer as a KBr pellet in the 4000−400 cm^{-1} range.

Preparation of $Ga_2Cu(SeO_3)_4$ (1). Blue rod-shaped single crystals were initially obtained by standard solid-state reaction. A mixture of CuCl (0.6 mmol), Ga_2O_3 (0.3 mmol), and SeO_2 (1.8 mmol) was thoroughly ground and pressed into a pellet, which was then sealed into an evacuated quartz tube. The quartz tube was heated at 440 °C for 7 days and cooled to 240 °C at 1.2 °C/h before the furnace was switched off. A few blue rod-shaped crystals of $Ga_2Cu(SeO_3)_4$ (**1**) were recovered from the reaction products composed of ternary gallium(III) selenite and copper(II) selenite. Some Cu(I) ions were oxidized to Cu(II) by SeO_2 during the reaction. Many attempts were made to prepare single-phase products for $Ga_2Cu(SeO_3)_4$ (**1**) by solid-state reactions or mild hydrothermal reactions of stoichiometric mixtures of CuO, Ga_2O_3, and SeO_2 at different temperatures, but the reaction products obtained were only a mixture of ternary copper(II) selenite and gallium(III) selenites.

Preparation of $Ga_2CuO(SeO_3)_3$ (2). Green block-shaped crystals were initially obtained by solid-state reactions of a mixture of $CuCl_2$ (0.5 mmol), Ga_2O_3 (0.5 mmol), and SeO_2 (1.5 mmol) at 500 °C for 3 days and cooling to 260 °C at 2.5 °C/h. EDS microprobe elemental analysis indicated the absence of chloride anion in the compound. The pure phase of $Ga_2CuO(SeO_3)_3$ (**2**) was directly prepared by heating stoichiometric amounts of CuO, Ga_2O_3, and SeO_2 at 560 °C. Its purity was confirmed by XRD powder diffraction studies. IR data (KBr cm^{-1}): 855(m), 760(s), 707(s), 641(m), 531(w), 430(w) (see Supporting Information).

Preparation of $Ga_2Cu_3(SeO_3)_6$ (3). Yellow-green brick-shaped crystals were initially obtained by standard solid-state reaction. A mixture of CuO (0.3 mmol), Ga_2O_3 (0.3 mmol), SeO_2 (1.8 mmol), and $CuCl_2$ (0.3 mmol) was heated at 535 °C for 5 days and cooled to 235 °C at 2 °C/h before the furnace was switched off. It is found that $CuCl_2$ played an important role in the synthesis of $Ga_2Cu_3(SeO_3)_6$ (**3**). Many attempts were made to prepare the pure phase of $Ga_2Cu_3(SeO_3)_6$ (**3**) by the direct solid-state reactions of corresponding stoichiometric mixtures of CuO, Ga_2O_3, and SeO_2 at different temperatures but failed. The samples used for IR, TGA, and magnetic measurements were prepared by mild hydrothermal reactions of a mixture of CuO (1.2 mmol), Ga_2O_3 (0.4 mmol), and SeO_2 (2.8 mmol) in 4 mL of H_2O sealed in an autoclave equipped with a Teflon liner (25 mL) at 200 °C for 7 days. Single crystals of $Ga_2Cu_3(SeO_3)_6$ (**3**) were collected in ca. 56% yield (based on Ga), and other products are colorless single crystals of gallium(III) selenite. It is found that a 15% excess of SeO_2 is necessary to obtain an optimum yield. Its purity was confirmed by XRD powder diffraction studies. IR data (KBr cm^{-1}): 859(m), 737(s), 686(m), 603(m), 546(m), 430(w) (see Supporting Information).

Preparation of $In_2Cu_3(SeO_3)_6$ (4). Green brick-shaped single crystals were initially obtained by mild hydrothermal reactions of a mixture of $CuCl_2 \cdot 2H_2O$ (1.0 mmol), In_2O_3 (0.5 mmol), SeO_2 (2.3 mmol), and H_2O (4 mL) at 200 °C for 7 days. The yield is ca. 32% based on In, and other products are colorless single crystals of indium(III) selenite. Its purity was confirmed by XRD powder diffraction studies. IR data (KBr cm^{-1}): 839(m), 746(s), 690(m), 649(m), 507(m), 434(w) (see Supporting Information).

X-ray Crystallography. Data collections were performed on either a Rigaku Mercury CCD diffractometer (for $Ga_2Cu(SeO_3)_4$ (**1**) and $M_2Cu_3(SeO_3)_6$ (M = Ga **3**, In **4**)) or a Rigaku Saturn70 CCD (for $Ga_2CuO(SeO_3)_3$ (**2**)) equipped with graphite-monochromated Mo Kα radiation (λ = 0.71073 Å) at 293 K. All four data sets were corrected for Lorentz and polarization factors. Absorption corrections by the multiscan method were applied.[14a] All four structures were solved by the direct methods and refined by full-matrix least-squares fitting on F^2 by SHELX-97.[14b] All atoms were refined with anisotropic thermal parameters. The data collection and refinement parameters are summarized in Table 1. Selected bond lengths are listed in Table 2. More details on the crystallographic studies as well as atomic displacement parameters are given as Supporting Information.

Results and Discussion

Solid-state or hydrothermal reactions of copper oxide or/and chloride (CuO, $CuCl_2$, CuCl), Ga_2O_3 or In_2O_3, and SeO_2 yielded four new copper(II), gallium(III)/indium(III) mixed metal selenites, namely, $Ga_2Cu(SeO_3)_4$ (**1**), $Ga_2CuO(SeO_3)_3$ (**2**), and $M_2Cu_3(SeO_3)_6$ (M = Ga **3**, In **4**). They represent the first examples of structurally characterized gallium(III)/indium(III) transition metal selenites.

(10) (a) Morris, R.-E.; Cheetham, A.-K. *Chem. Mater.* **1994**, *6*, 67. (b) Dutreilh, M.; Thomas, P.; Champarnaud-Mesjard, J.-C.; Frit, B. *Solid State Sci.* **2001**, *3*, 423.

(11) (a) Yu, R.; Ok, K.-M.; Halasyamani, P.-S. *Dalton Trans.* **2004**, 392. (b) Paterson, B.; Harrison, W. T. A. *Z. Anorg. Allg. Chem.* **2007**, *633*, 158.

(12) (a) Miletich, R.; Pertlik, F. *J. Alloys. Compd.* **1998**, *268*, 107. (b) Bhuvanesh, N. S. P.; Halasyamani, P.-S. *Inorg. Chem.* **2001**, *40*, 1404.

(13) (a) Ok, K.-M.; Halasyamani, P.-S. *Chem. Mater.* **2001**, *13*, 4278. (b) Ok, K.-M.; Halasyamani, P.-S. *Chem. Mater.* **2002**, *14*, 2360.

(14) (a) *CrystalClear*, Version 1.3.5; Rigaku Corp.: The Woodlands, TX, **1999**. (b) Sheldrick, G. M. *SHELXTL, Crystallographic Software Package*, Version 5.1; Bruker-AXS: Madison, WI, **1998**.

Table 1. Crystal Data and Structure Refinements for **1**−**4**

	1	**2**	**3**	**4**
formula	$Ga_2Cu(SeO_3)_4$	$Ga_2CuO(SeO_3)_3$	$Ga_2Cu_3(SeO_3)_6$	$In_2Cu_3(SeO_3)_6$
fw	742.82	599.86	1091.82	1182.02
space group	*P*2(1)/*c* (No. 14)	*Pmna* (No. 53)	*P*2(1)/*c* (No. 14)	*P*2(1)/*c* (No. 14)
a (Å)	16.976(2)	6.495(2)	12.269(4)	5.4927(15)
b (Å)	4.5881(2)	9.598(3)	8.186(3)	19.278(5)
c (Å)	14.902(1)	13.443(5)	7.594(2)	9.2318(18)
α (deg)	90	90	90	90
β (deg)	115.493(3)	90	95.895(6)	123.432(11)
γ (deg)	90	90	90	90
V (Å^3)	1047.7(1)	838.0(5)	758.7(4)	815.8(3)
Z	4	4	2	2
D_{calc} (g cm^3)	4.709	4.755	4.779	4.812
μ(Mo Kα) (mm^{-1})	21.104	21.973	22.140	20.114
GOF on F^2	0.940	1.046	1.023	1.070
R_1, wR_2 ($I > 2\sigma(I)$)[a]	0.0278, 0.0639	0.0213, 0.0583	0.0222, 0.0545	0.0224, 0.0534
R_1, wR_2 (all data)[a]	0.0345, 0.0686	0.0256, 0.0604	0.0264, 0.0570	0.0250, 0.0547

[a] $R_1 = \sum||F_o| - |F_c||/\sum|F_o|$, $wR_2 = \{\sum w[(F_o)^2 - (F_c)^2]^2/\sum w[(F_o)^2]^2\}^{1/2}$.

The asymmetric unit of $Ga_2Cu(SeO_3)_4$ (**1**) contains two copper(II) atoms located at the inversion centers, two gallium(III) and four selenite anions in the general sites. The coordination geometries around both Cu(1) and Cu(2) can be described as a "4+2" Jahn−Teller distorted octahedron. The axial Cu−O bond length [2.425(4)−2.447(4) Å] is significantly longer than the basal Cu−O bonds [1.943(3)−1.988(4) Å]. Both Ga(1) and Ga(2) are octahedrally coordinated by six selenite oxygen atoms with Ga−O distances in the range 1.859(4)−2.133(4) Å. All four Se(IV) atoms are in ψ-SeO_3 trigonal pyramidal geometry with the lone pairs of Se(IV) occupying the pyramidal sites. The selenite groups are isolated from each other, and the Se−O bond distances are in the range 1.675(4)−1.730(4) Å. Bond valence calculations indicate that Cu, Ga, and Se atoms are in an oxidation state of +2, +3, and +4, respectively. The calculated total bond valences for Ga(1), Ga(2), Cu(1), Cu(2), Se(1), Se(2), Se(3), and Se(4) are 3.07, 3.05, 2.05, 2.06, 3.96, 4.05, 3.98, and 4.08, respectively.[15]

$Ga_2Cu(SeO_3)_4$ (**1**) contains a 2D layer of corner-shared GaO_6 and CuO_6 octahedra with the SeO_3 groups hanging on both sides (Figure. 1). Neighboring GaO_6 octahedra are interconnected to a 1D zigzag chain along the *b*-axis via corner-sharing, and such chains are further bridged by the CuO_6 octahedra into a 2D infinite layer via corner-sharing. The SeO_3 groups are grafted on the two sides of the 2D layer (Figure 2). The nearest Cu···Cu separation between Cu(II) ions bridged by a GaO_6 octahedron is 4.563 Å. The Se(1)O_3 and Se(3)O_3 anions are tetradentate metal linkers, forming a four-membered chelating ring with a Ga(III) ion and also bridged to two other Ga(III) and one Cu(II) ion. The Se(2)O_3 and Se(4)O_3 anions are tridentate metal linkers, forming a bidentate chelation with a Cu(II) ion and also bridging with two Ga(III) atoms. The lone-pair electrons of the Se(IV) cations are orientated toward the interlayer space. The interlayer distance is 8.49 Å, which is half of the *a*-axis length.

The asymmetric unit of $Ga_2CuO(SeO_3)_3$ (**2**) contains one Cu(II) atom, two Ga(III) atoms, and three Se(IV) atoms. Cu and Ga(1) are in the site of C_2 symmetry, whereas Ga(2), Se(1), Se(2), and Se(3) are located at the sites of *m* symmetry. The Cu^{2+} ion is octahedrally coordinated by six selenite oxygen atoms with Cu−O distances in the range 1.921(3)−2.214(3) Å. Ga(1) is tetrahedrally coordinated with four oxygen atoms, two of which from selenite groups and the other two from two O^{2-} anions. Ga(2) is five-coordinated with five oxygen atoms in a square pyramidal geometry, four oxygens from selenite groups and one from O^{2-} anion. Most of the Ga−O distances fall in the range 1.810(2)−1.978(3) Å except Ga(2)−O(7) of 2.222(4) Å in the Ga(2)O_5 square pyramid. All three Se(IV) atoms are in ψ-SeO_3 trigonal pyramidal geometries with the lone pairs of Se(IV) occupying the pyramidal sites. The Se−O distances range from 1.678(3) to 1.738(4) Å. Bond valence calculations indicate that the Cu, Ga, and Se atoms are in an oxidation state of +2, +3, and +4, respectively. The calculated total bond valences for Ga(1), Ga(2), Cu, Se(1), Se(2), and Se(3) are 2.87, 2.63, 2.22, 4.093, 4.060, and 4.033, respectively.[15]

$Ga_2CuO(SeO_3)_3$ (**2**) features a pillared layered structure in which the 1D $[Cu(SeO_3)_3]^{4-}$ chains act as the pillars between 2D layers formed by corner- and edge-sharing GaO_n (n=4, 5) polyhedra (Figure 3). The CuO_6 octahedra are interconnected via edge-sharing [O(3)···O(4)] into a 1D chain along the *a*-axis. The Cu···Cu separation between the two edge-shared CuO_6 octahedra is 3.234(1) Å. The Cu−O(3)−Cu and Cu−O(4)−Cu bond angles are 103.8(2)° and 94.4(2)°, respectively. The selenite groups are hanging on the chain in a unidentate or bidentate fashion (Figure 4a). Two Ga(2)O_5 square pyramids are interconnected via edge-sharing [O(7)···O(7)] to form a Ga_2O_8 dimeric unit, whereas Ga(1)-O_4 tetrahedra form a 1D chain along the *a*-axis via corner-sharing. Neighboring tetrahedral chains are bridged by Ga_2O_8 dimers via corner-sharing into a 2D layer parallel to the *ac*-plane, forming 8-MRs composed of two Ga_2O_8 dimers and four Ga(1)O_4 tetrahedra (Figure 4b). The above gallium(III) oxide layers and copper(II) selenite chains are further interconnected via Se−O−Ga bridges into a 3D network. All of the SeO_3^{2-} anions are tetradentate metal linkers, bridging with two Ga(III) ions and two Cu(II) atoms. The lone pair electrons of the Se(IV) cations are orientated toward the voids of the structure (Figure 3).

The structure of $Ga_2Cu_3(SeO_3)_6$ (**3**) features a complicated 3D network (Figure 5). The asymmetrical unit contains one gallium(III), two copper(II), and three selenium(IV) atoms with Cu(1) on an inversion center. The gallium(III) ion is octahedrally coordinated with six oxygen atoms from selenite

(15) (a) Brown, I. D.; Altermatt, D. *Acta Crystallogr.* **1985**, *B41*, 244. (b) Brese, N. E.; O'Keeffe, M. *Acta Crystallogr.* **1991**, *B47*, 192.

Table 2. Important Bond Lenghts (Å) for **1**−**4**[a]

	$Ga_2Cu(SeO_3)_4$ (**1**)		
Ga(1)−O(4)	1.895(4)	Ga(1)−O(5)#1	1.919(4)
Ga(1)−O(2)#2	1.920(4)	Ga(1)−O(1)	2.021(4)
Ga(1)−O(3)#3	2.069(4)	Ga(1)−O(3)	2.095(4)
Ga(2)−O(11)	1.911(4)	Ga(2)−O(8)	1.916(4)
Ga(2)−O(10)#1	1.918(4)	Ga(2)−O(9)#4	2.007(4)
Ga(2)−O(7)#5	2.054(3)	Ga(2)−O(7)#4	2.133(4)
Cu(1)−O(1)	1.969(4)	Cu(1)−O(1)#6	1.969(4)
Cu(1)−O(6)	1.988(4)	Cu(1)−O(6)#6	1.988(4)
Cu(1)−O(5)	2.425(4)	Cu(1)−O(5)#6	2.425(4)
Cu(2)−O(9)	1.943(3)	Cu(2)−O(9)#7	1.943(3)
Cu(2)−O(12)#8	1.998(4)	Cu(2)−O(12)#9	1.998(4)
Cu(2)−O(10)#8	2.477(4)	Cu(2)−O(10)#9	2.477(4)
Se(1)−O(2)	1.675(4)	Se(1)−O(1)	1.722(4)
Se(1)−O(3)	1.730(4)	Se(2)−O(6)	1.687(4)
Se(2)−O(4)	1.706(4)	Se(2)−O(5)	1.708(4)
Se(3)−O(8)	1.676(4)	Se(3)−O(9)	1.722(4)
Se(3)−O(7)	1.724(4)	Se(4)−O(12)	1.684(4)
Se(4)−O(10)	1.704(4)	Se(4)−O(11)	1.705(4)
	$Ga_2CuO(SeO_3)_3$ (**2**)		
Ga(1)−O(1)	1.810(2)	Ga(1)−O(1)#1	1.810(2)
Ga(1)−O(2)#2	1.902(3)	Ga(1)−O(2)	1.902(3)
Ga(2)−O(1)	1.864(4)	Ga(2)−O(7)#3	1.893(4)
Ga(2)−O(5)#4	1.978(3)	Ga(2)−O(5)#5	1.978(3)
Ga(2)−O(7)#6	2.222(4)	Cu−O(6)#2	1.921(3)
Cu−O(6)	1.921(3)	Cu−O(3)	2.063(2)
Cu−O(3)#1	2.063(2)	Cu−O(4)#1	2.214(3)
Cu−O(4)	2.214(3)	Se(1)−O(2)	1.678(3)
Se(1)−O(2)#7	1.678(3)	Se(1)−O(3)	1.735(4)
Se(2)−O(5)	1.681(3)	Se(2)−O(5)#7	1.681(3)
Se(2)−O(4)	1.738(4)	Se(3)−O(6)#7	1.694(3)
Se(3)−O(6)	1.694(3)	Se(3)−O(7)	1.717(4)
	$Ga_2Cu_3(SeO_3)_6$ (**3**)		
Ga−O(7)	1.920(3)	Ga−O(8)#1	1.929(3)
Ga−O(9)#2	1.959(3)	Ga−O(1)#3	1.985(3)
Ga−O(5)#4	2.033(3)	Ga−O(3)	2.099(3)
Cu(1)−O(4)	1.940(3)	Cu(1)−O(4)#5	1.940(3)
Cu(1)−O(6)#3	2.013(3)	Cu(1)−O(6)#6	2.013(3)
Cu(1)−O(2)#5	2.368(3)	Cu(1)−O(2)	2.368(3)
Cu(2)−O(3)	1.935(3)	Cu(2)−O(6)	1.969(3)
Cu(2)−O(2)#7	2.004(3)	Cu(2)−O(4)	2.060(3)
Cu(2)−O(5)#4	2.216(3)	Se(1)−O(1)	1.688(3)
Se(1)−O(2)	1.689(3)	Se(1)−O(3)	1.739(3)
Se(2)−O(5)	1.691(3)	Se(2)−O(6)	1.732(3)
Se(2)−O(4)	1.741(3)	Se(3)−O(9)	1.698(3)
Se(3)−O(8)	1.700(3)	Se(3)−O(7)	1.714(3)
	$In_2Cu_3(SeO_3)_6$ (**4**)		
In(1)−O(3)	2.101(3)	In(1)−O(1)#1	2.119(3)
In(1)−O(2)#2	2.133(3)	In(1)−O(6)	2.141(3)
In(1)−O(9)	2.158(3)	In(1)−O(4)	2.252(3)
Cu(1)−O(4)#3	1.970(3)	Cu(1)−O(4)	1.970(3)
Cu(1)−O(8)#4	1.975(3)	Cu(1)−O(8)#5	1.975(3)
Cu(2)−O(5)#6	1.919(3)	Cu(2)−O(7)#4	1.953(3)
Cu(2)−O(7)#7	1.964(3)	Cu(2)−O(8)	2.013(3)
Cu(2)−O(9)#4	2.239(3)	Se(1)−O(1)	1.690(3)
Se(1)−O(2)	1.692(3)	Se(1)−O(3)	1.698(3)
Se(2)−O(5)	1.683(3)	Se(2)−O(9)#7	1.722(3)
Se(2)−O(4)	1.743(3)	Se(3)−O(6)	1.681(3)
Se(3)−O(8)	1.718(3)	Se(3)−O(7)	1.722(3)

[a] Symmetry transformations used to generate equivalent atoms: For **1**: #1 $x, y+1, z$; #2 $-x+1, y+1/2, -z+1/2$; #3 $-x+1, y-1/2, -z+1/2$; #4 $-x, y-1/2, -z-1/2$; #5 $x, y-1, z$. #6 $-x+1, -y+1, -z$; #7 $-x, -y+2, -z-1$; #8 $x, -y+3/2, z-1/2$; #9 $-x, y+1/2, -z-1/2$. For **2**: #1 $x+1/2, y, -z+1/2$; #2 $-x+1/2, y, -z+1/2$; #3 $x, y-1, z$; #4 $x-1/2, y-1, -z+1/2$; #5 $-x+1/2, y-1, -z+1/2$; #6 $-x, -y+1, -z+1$; #7 $-x, y, z$. For **3**: #1 $-x, -y+1, -z$; #2 $-x, y-1/2, -z-1/2$; #3 $x, -y+3/2, z-1/2$; #4 $-x+1, -y+1, -z$; #5 $-x+1, -y+2, -z$; #6 $-x+1, y+1/2, -z+1/2$; #7 $x, -y+3/2, z+1/2$. For **4**: #1 $x+1, y, z$; #2 $x, -y-1/2, z-1/2$; #3 $-x, -y, -z$; #4 $-x+1, -y, -z+1$; #5 $x-1, y, z-1$; #6 $x+1, y, z+1$; #7 $x-1, y, z$.

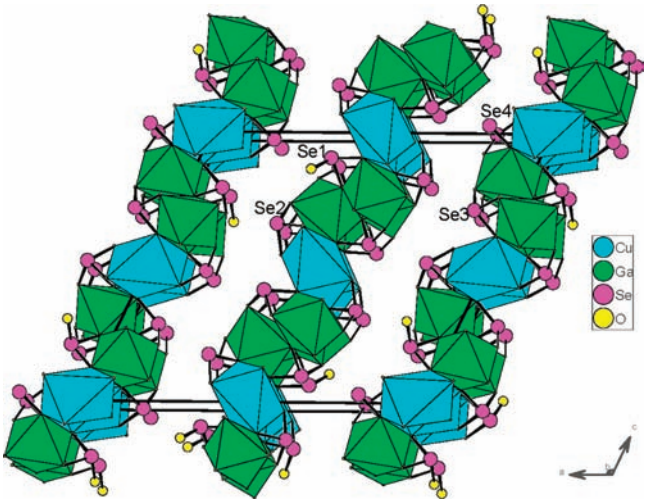

Figure 1. View of the structure of $Ga_2Cu(SeO_3)_4$ (**1**) down the *b*-axis. The CuO_6 and GaO_6 octahedra are drawn as cyan and green, respectively. Se and O atoms are drawn as pink and yellow circles, respectively.

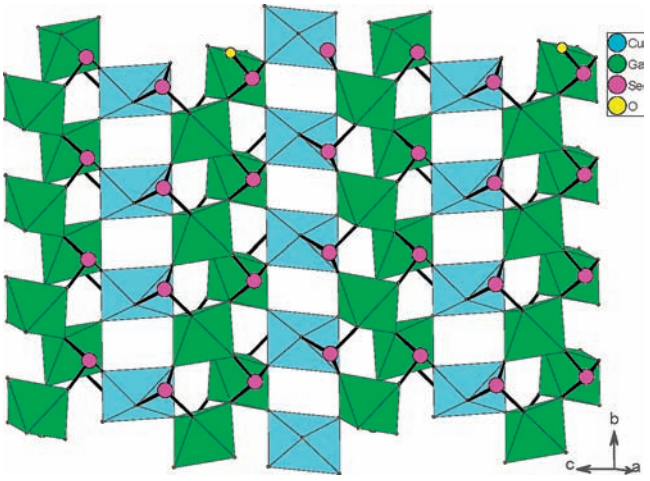

Figure 2. Gallium(III) copper(II) selenite layer in $Ga_2Cu(SeO_3)_4$ (**1**). CuO_6 and GaO_6 octahedra are drawn as cyan and green, respectively. Se and O atoms are drawn as pink and yellow circles, respectively.

groups with Ga−O distances in the range 1.920(3)−2.099(3) Å. The coordination geometry around Cu(1) can be described as a "4+2" Jahn−Teller distorted octahedron. The axial Cu−O bond length of 2.368(3) Å is significantly longer than the basal ones [1.940(3)−2.013(3) Å]. The coordination geometry around Cu(2) is a distorted square pyramid, exhibiting a "4 + 1" coordination with four normal [1.935(3)−2.060(3) Å] and one elongated [2.216(3) Å] Cu−O bond. All three Se(IV) atoms are in ψ-SeO_3 trigonal pyramidal geometries with the lone pairs occupying the pyramidal sites. The Se−O bond distances are in the range 1.688(3)−1.741(3) Å, which are comparable to those reported in other metal selenites.[1] Bond valence calculations indicate that the Cu, Ga, and Se atoms are in an oxidation state of +2, +3, and +4, respectively. The calculated total bond valences for Ga, Cu(1), Cu(2), Se(1), Se(2), and Se(3) are 3.03, 2.11, 1.96, 4.00, 3.83, and 4.01, respectively.[15]

$Ga_2Cu_3(SeO_3)_6$ (**3**) displays a pillared layered structure built of $[Ga_2Cu_3(SeO_3)_4]^{4+}$ thick layers and $Se(3)O_3^{2-}$ anions as the pillars (Figure 5). One $Cu(1)O_6$ octahedron and two

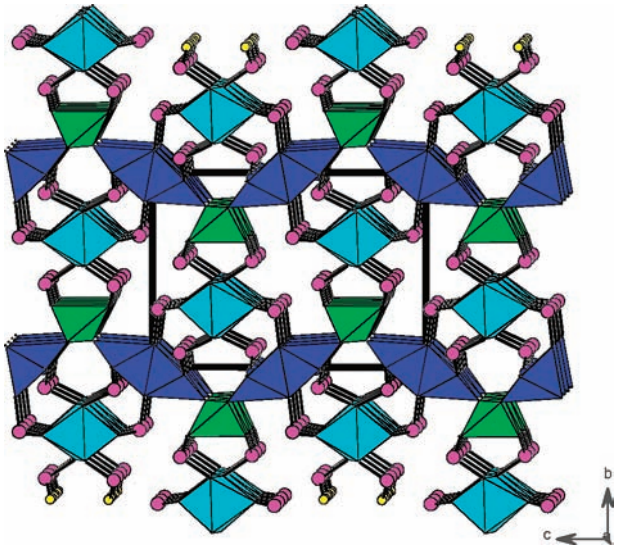

Figure 3. View of the 3D network structure of $Ga_2CuO(SeO_3)_3$ (**2**) down the *a*-axis. CuO_6, GaO_4 tetrahedra, and GaO_5 square pyramids are shaded in cyan, green, and blue, respectively. Se and O atoms are drawn as pink and yellow circles, respectively.

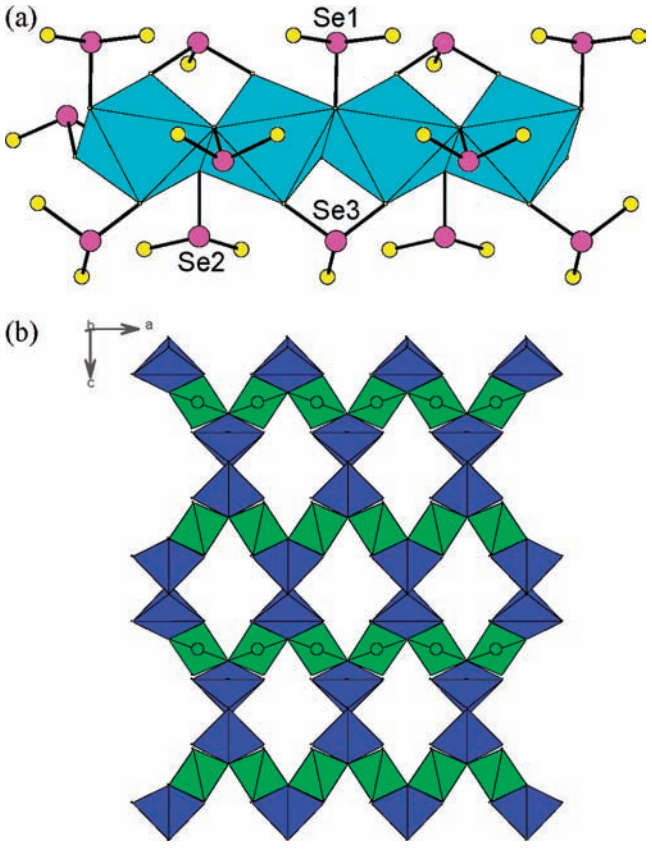

Figure 4. Copper(II) selenite chain along the *a*-axis (a) and a gallium-(III) oxide layer perpendicular to the *b*-axis (b) in $Ga_2CuO(SeO_3)_3$ (**2**). CuO_6, GaO_4 tetrahedra, and GaO_5 square pyramids are shaded in cyan, green, and blue, respectively. Se and O atoms are drawn as pink and yellow circles, respectively.

$Cu(2)O_5$ square pyramids are interconnected via O(2)···O(6) corner-sharing to form a linear trimer. Each trimer further connects with four neighbors via corner-sharing O(4), resulting in the formation of a 2D copper(II) oxide layer parallel to the *bc*-plane with long, narrow shaped eight-membered rings (Figure 6). The Cu···Cu separation between two edge-sharing CuO_x (x = 5, 6) polyhedra is 3.2119(8) Å, and that between corner-sharing ones is 3.6098(8) Å. The Cu(1)−O(2)−Cu(2), Cu(1)−O(6)−Cu(2), and Cu(1)−O(4)−Cu(2) bond angles are 94.2(1)°, 107.6(1)°, and 128.9(1)°, respectively. The GaO_6 octahedra are attached on both sides of the copper(II) oxide layer via edge-sharing. The $Se(1)O_3$ anions are hanging on the layer, whereas the $Se(2)O_3$ groups are located at the voids within the layer, resulting in a thick $[Ga_2Cu_3(SeO_3)_4]^{4+}$ layer. The thickness of the layer is about 10.3 Å. The $Se(3)O_3$ groups further cross-link above thick Ga−Cu−Se−O layers into a complicated 3D network (Figure 5). The selenite anions adopt three different coordination modes. The $Se(1)O_3$ group is a pentadentate metal linker, connecting with three Cu(II) ions and two Ga(III) ions, whereas the $Se(2)O_3$ anion is a hexadentate metal linker, forming a four-membered chelating ring with a Cu(II) ion and also bridging to three other Cu(II) ions and one Ga(III) ion. The $Se(3)O_3$ group is a tridentate metal linker, bridging to three Ga(III) ions. The lone pairs of these selenite anions are orientated toward the voids of the 3D network (Figure 5).

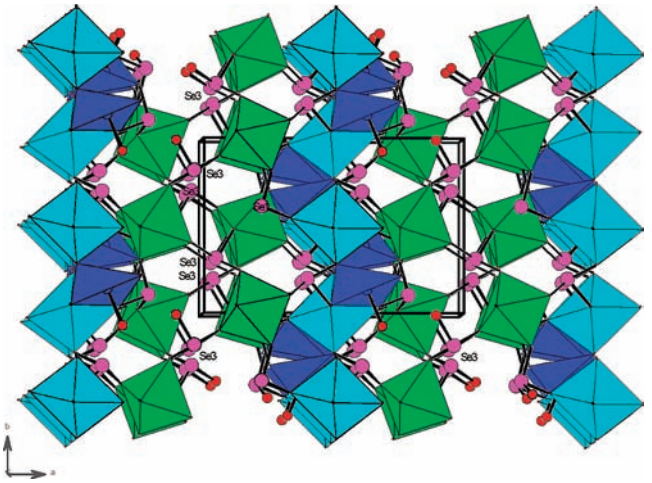

Figure 5. View of the 3D network structure of $Ga_2Cu_3(SeO_3)_6$ (**3**) down the *c*-axis. CuO_6 octahedra, CuO_5 square pyramids, and GaO_6 octahedra are drawn as cyan, blue, and green, respectively. Se and O atoms are drawn as pink and yellow circles, respectively.

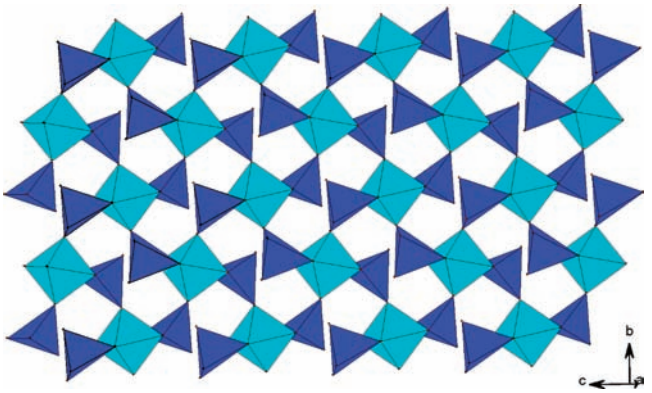

Figure 6. View of the Cu−O layer in $Ga_2Cu_3(SeO_3)_6$ (**3**). CuO_6 octahedra and CuO_5 square pyramids are shaded in cyan and blue, respectively.

When the indium(III) oxide was used instead of gallium-(III) oxide, $In_2Cu_3(SeO_3)_6$ (**4**) was isolated. Although its

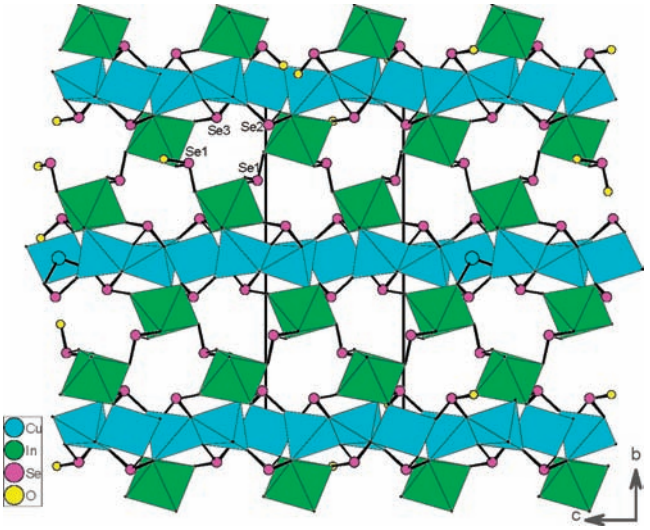

Figure 7. View of structure of $In_2Cu_3(SeO_3)_6$ (**4**) down the *a*-axis. CuO_5 square pyramids and GaO_6 octahedra are drawn as cyan and green, respectively. Se and O atoms are drawn as pink and yellow circles, respectively.

chemical composition is comparable to that of $Ga_2Cu_3(SeO_3)_6$ (**3**), it exhibits a completely different structure.

The asymmetric unit of $In_2Cu_3(SeO_3)_6$ (**4**) is composed of one In(III) and two Cu(II) ions as well as three SeO_3^{2-} anions. The indium(III) is octahedrally coordinated with six oxygen atoms from selenite anions with the distances of In−O ranging from 2.101(3) to 2.252(3) Å. The two Cu(II) ions exhibit two types of coordination geometries. Cu(1) located on an inversion center is in a square planar coordination geometry with the Cu−O distances in the range 1.970(3)−1.975(3) Å. The *trans* O−Cu−O angles are 180°, whereas those of *cis* O−Cu−O are 88.1(1)° and 91.9(1)°. The coordination geometry around Cu(2) is a distorted square pyramid, showing a "4 + 1" coordination with four normal [1.919(3)−2.013(3) Å] and one elongated [2.239(3) Å] Cu−O bond, which are comparable to those in $Ga_2Cu_3(SeO_3)_6$ (**3**). All three Se(IV) atoms are in ψ-SeO_3 trigonal pyramidal geometries with the lone pairs of Se(IV) occupying the pyramidal sites. The Se−O bond distances are in the range 1.681(3)−1.743(3) Å, which are comparable to those reported in $Ga_2Cu_3(SeO_3)_6$ (**3**). Bond valence calculations indicate that the Cu, In, and Se atoms are in an oxidation state of +2, +3, and +4, respectively. The calculated total bond valences for In, Cu(1), Cu(2), Se(1), Se(2), and Se(3) are 3.09, 1.81, 2.09, 4.12, 3.89, and 3.98, respectively.[15]

The structure of $In_2Cu_3(SeO_3)_6$ (**4**) features a 3D network composed of a copper(II) selenite layer and corrugated indium(III) selenite layer with 8-MR helical tunnels along the *a*-axis (Figure 7). The lone pairs of the selenite anions are orientated toward the above tunnels. The InO_6 octahedra are bridged by $Se(1)O_3$ and $Se(2)O_3$ groups into a corrugated 2D layer passing through about 1/4 and 3/4 of the *b*-axis (Figure 8a). A pair of $Cu(2)O_5$ square pyramids are interconnected to a $[Cu_2O_8]^{12-}$ dimer via edge-sharing of O(7)···O(7). Neighboring dimers are further bridged by the $Cu(1)O_4$ squares into a 1D Cu−O chain via corner-sharing O(8). Such 1D chains are further bridged by $Se(2)O_3$ and $Se(3)O_3$ groups into a 2D layer (Figure 8b). The Cu···Cu separations between two edge-sharing copper(II) coordination polyhedra are 3.0495(9) Å, and those between the

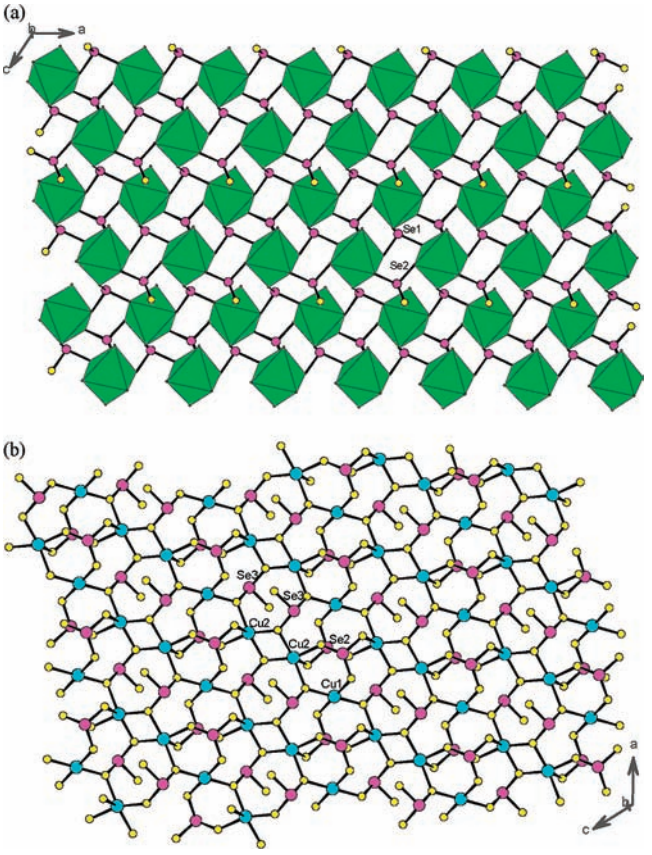

Figure 8. Indium(III) selenite layer (a) and a copper(II) selenite layer (b) in $In_2Cu_3(SeO_3)_6$ (**4**). InO_6 octahedra are shaded in green. Cu, Se, and O atoms are drawn as cyan, pink, and yellow circles, respectively.

corner-sharing ones are 3.3896(1) Å. The shortest interchain Cu···Cu separation is 4.1025(1) Å. The Cu(2)−O(7)−Cu(2) and Cu(1)−O(8)−Cu(2) bond angles are 102.9(1)° and 115.6(1)°, respectively. The corrugated indium(III) selenite layers and the copper(II) selenite layers are interconnected and alternate along the *b*-axis into a 3D network through Se−O−Cu and In−O−Cu bridges, forming 8-MR helical tunnels along the *a*-axis (Figure 7). The selenite anions adopt three different types of coordination modes. The $Se(1)O_3$ group is a tridentate metal linker, bridging to three In(III) ions, whereas the $Se(2)O_3$ group is a pentadentate metal linker, bridging with three Cu(II) ions and two Ga(III) ions. The $Se(3)O_3$ group is also a pentadentate metal linker, but bridging with four Cu(II) ions and one Ga(III) ion.

Although the chemical composition of $M_2Cu_3(SeO_3)_6$ (M = Ga **3**, In **4**) is comparable to that of $Tl_2Cu_3(SeO_3)_6$, each of them forms a unique structural type.[16] In $Tl_2Cu_3(SeO_3)_6$, the Tl(III) ion is seven-coordinated with seven selenite oxygen atoms. Two TlO_7 polyhedra are interconnected into a dimer via edge-sharing, and a pair of CuO_6 octahedra also forms a dimer via corner-sharing. The above two types of dimers are further interconnected via edge-sharing into a 1D chain along the *c*-axis. Neighboring chains are cross-linked by bridging selenite groups into a 2D layer parallel to the *ac*-plane. These neighboring layers are further bridged by CuO_4 squares into a 3D network with 12-MR tunnels along the *a*-axis.[16]

TGA and IR Analyses. TGA analyses under an air atmosphere indicate that $Ga_2CuO(SeO_3)_3$ (**2**), $Ga_2Cu_3(SeO_3)_6$ (**3**),

(16) Giester, G. *Z. Kristallogr.* **1999**, *214*, 305.

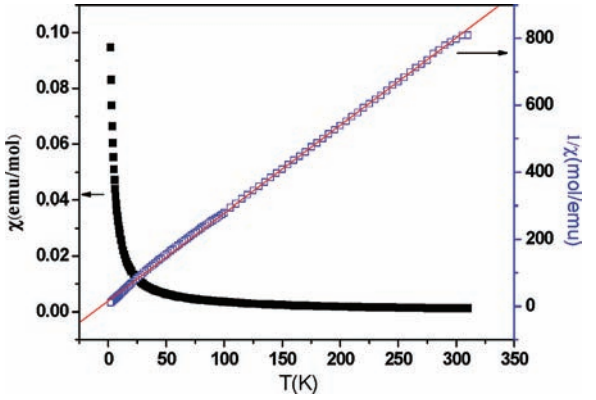

Figure 9. χ and $1/\chi$ vs T plots for $Ga_2CuO(SeO_3)_3$ (**2**). The solid line corresponds to the fitting according to the Curie−Weiss law.

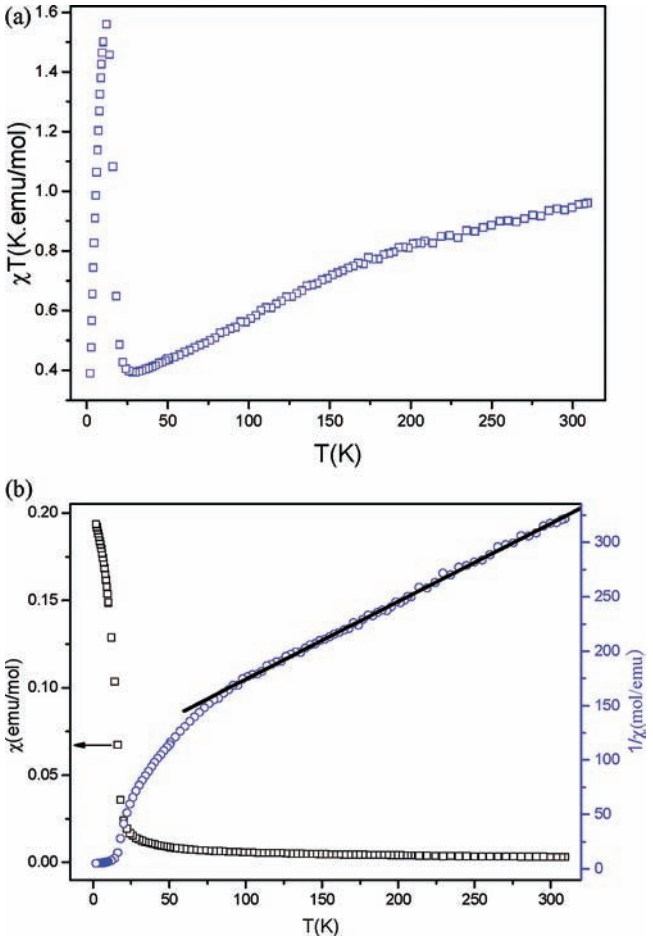

Figure 10. χT vs T plot (a) and the χ and $1/\chi$ vs T plots (b) for $Ga_2Cu_3(SeO_3)_6$ (**3**). The solid line corresponds to the fitting according to the Curie−Weiss law.

and $In_2Cu_3(SeO_3)_6$ (**4**) are stable up to ca. 330, 440, and 450 °C, respectively (see Supporting Information). The weight loss in the temperature ranges 330−600, 440−605, and 450−690 °C, respectively, for $Ga_2CuO(SeO_3)_3$ (**2**), $Ga_2Cu_3(SeO_3)_6$ (**3**), and $In_2Cu_3(SeO_3)_6$ (**4**) correspond to the release of 3, 6, and 6 mol of SeO_2 per formula unit.[5] The observed weight losses of 44.9%, 61.3%, and 55.7% at 1000 °C respectively for $Ga_2CuO(SeO_3)_3$ (**2**), $Ga_2Cu_3(SeO_3)_6$ (**3**), and $In_2Cu_3(SeO_3)_6$ (**4**) are close to the calculated ones (44.5%, 61.0%, and 56.3%, respectively). The final residuals were not characterized due to their melting with the TGA bucket made of Al_2O_3 under such high temperature. The IR spectra of the three compounds are similar. They are transparent in the range 4000−1000 cm^{-1}. The absorption bands in the region from 860 to 650 cm^{-1} are characteristic of ν(Se−O) stretching vibrations, and the bands in the range 550−430 cm^{-1} can be assigned to ν(O−Se−O) bending vibrations (see Supporting Information). All of the assignments are consistent with those previously reported.[17]

Magnetic Properties. The temperature-dependent magnetic susceptibilities of $Ga_2CuO(SeO_3)_3$ (**2**) and $M_2Cu_3(SeO_3)_6$ (M = Ga **3**, In **4**) were measured at 5 kOe in the temperature range 2−300 K.

The χ and $1/\chi$ vs T plots for $Ga_2CuO(SeO_3)_3$ (**2**) are shown in Figure 9. The value of χT at 300 K is 0.376 emu mol^{-1} K, which corresponds to the expected value for one isolated Cu(II) ion ($\chi_{Cu}T = 0.375$ emu mol^{-1} K and $S = 1/2$). It decreases continuously with cooling and reaches 0.189 emu mol^{-1} K at 2 K, indicating dominant antiferromagnetic interaction between copper(II) centers. Fitting of $1/\chi$ in the temperature range 300−2 K according to Curie−Weiss law gave $C = 0.38$ emu mol^{-1} K and $\theta = -6.3$ K. The negative sign of the Curie−Weiss constant indicates the dominant antiferromagnetic interaction between Cu(II) centers.

The χT, χ, and $1/\chi$ vs T plots for $Ga_2Cu_3(SeO_3)_6$ (**3**) are shown in Figure 10. The value of χT at 300 K is 0.94 emu mol^{-1} K, which is smaller than the value expected for three isolated Cu(II) ions ($3\chi_{Cu}T = 1.125$ emu mol^{-1} K and $S = 1/2$). Upon cooling, χT decreases smoothly and reaches a minimum of 0.39 emu mol^{-1} K at ca. 30 K. Below 30 K, χT increases abruptly and reaches a maximum at ca. 12 K (χT_{max} = 1.56 emu mol^{-1} K) and finally decreases again at lower temperatures, indicating a magnetic phase transition. The temperature dependence of $1/\chi$ between 300 and 80 K agrees with the Curie−Weiss behavior with $C = 1.4$ emu mol^{-1} K and $\theta = -143.8$ K. The negative sign of the Curie−Weiss constant indicates strong antiferromagnetic interaction between Cu(II) centers.

The increase in $\chi_M T$ observed at low temperatures corresponds to the onset of a weak ferromagnetic ordering due to spin canting of the antiferromagnetically coupled Cu(II) ions.[18] The ordering was verified by the divergence of zero-field-cooled (ZFC) and field-cooled (FC) susceptibility (Figure 11a) at low temperature. The divergence of direct-current ZFC and FC samples reveals the history dependence of the magnetization process. Furthermore, the susceptibility below 16 K is field-dependent, as shown in Figure 11b, consistent with the spin canting. The zero-field ac magnetic susceptibility measurement under $H_{ac} = 3$ Oe at different frequencies shows both in-phase [$\chi_M'(T)$] and out-of-phase [$\chi_M''(T)$] signals with peaks appearing at T_c of ca. 15 K, which is frequency-independent (Figure 11c). This confirms the onset of a long-range ferromagnetic-like ordering at low temperature. The field dependence of the magnetization,

(17) (a) Porter, Y.; Halasyamani, P.-S. *Inorg. Chem.* **2003**, *42*, 205. (b) Nyquist, R. A.; Kagel, R. O. *Infrared Spectra of Inorganic Compounds*; Academic Press: New York, 1971.

(18) (a) Carlin, R. L. *Magnetochemistry*; Springer-Verlag: Berlin, 1986. (b) Kahn, O. Molecular Magnetism; VCH: Weinheim, 1993.

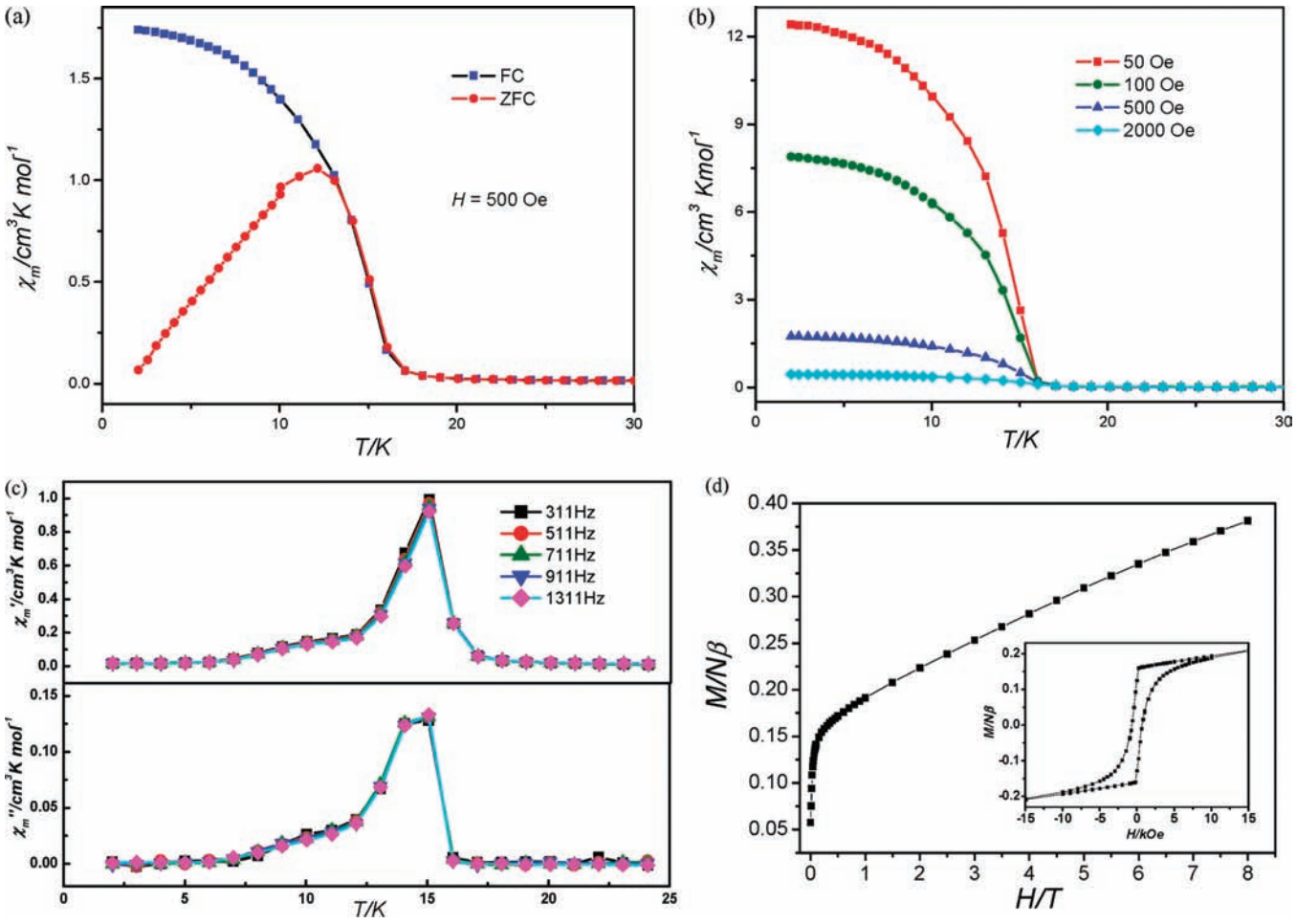

Figure 11. Zero-field-cooled (ZFC) and field-cooled (FC) magnetization (a), temperature dependence of χ_M at different fields (b), temperature dependence of ac magnetic susceptibilities at different frequencies (c), and field dependence of magnetization and hysteresis loop (inset) at 2 K (d) for $Ga_2Cu_3(SeO_3)_6$ (**3**).

$M(H)$, at 2 K (Figure 11d) shows an abrupt increase of the magnetization at fields below 800 Oe and a steady increase from above 800 Oe and reaches 0.38 Nβ at 8 T, without achieving saturation. The hysteresis loops measured at 2 K are consistent with a weak ferromagnetism (Figure 11d, inset). The coercive field is ca. 700 Oe, which is characteristic for a soft magnet. The remnant magnetization is 0.1253. The spontaneous magnetization observed is due to spin canting, with an estimated large canting angle of 7.1°. This angle is calculated by using the equation $\psi = \tan^{-1}(M_r/M_s)$, where M_r is the remnant magnetization and $M_s = gS$ is the expected saturation magnetization if all of the moments are aligned ferromagnetically.[19] Among the reported molecular weak ferromagnets, those with canting angles larger than 7.1° are still limited.[20−23]

It is well known that the occurrence of spin canting is usually caused by either single-ion magnetic anisotropy or antisymmetric exchange in magnetic entities. In $Ga_2Cu_3(SeO_3)_6$ (**3**), the observed spin canting may be attributed to the antisymmetric magnetic exchange, which is related to the symmetry of the magnetic entities. Seemingly, it is not compatible with the centric structure of $Ga_2Cu_3(SeO_3)_6$ (**3**). Actually, the axes passing through the metal centers of the linear trinuclear units composed of a $Cu(1)O_6$ octahedron edge-sharing with two $Cu(2)O_5$ square pyramids are not parallel within the copper(II) oxide layer, which means that they are tilted with respect to each other and the spins do not completely cancel (Figure 12). Although canted antiferromagnetism has been observed in some metal coordination complexes, it is not common for Cu(II) systems, except for several recently reported examples.[24,25]

(19) (a) Palacio, F.; Andres, M.; Horne, R.; van Duyneveldt, A. J. *J. Magn. Magn. Mater.* **1986**, *54*−*57*, 1487. (b) Marvilliers, A.; Parsons, S.; Riviere, E.; Audiere, J.-P.; Kurmoo, M.; Mallah, T. *Eur. J. Inorg. Chem.* **2001**, 1287.

(20) (a) Wang, X. Y.; Wang, L.; Wang, Z. M.; Gao, S. *J. Am. Chem. Soc.* **2006**, *128*, 674. (b) Wang, X.-Y.; Wang, Z.-M.; Gao, S. *Inorg. Chem.* **2008**, *47*, 5720.

(21) (a) Batten, S. R.; Murray, K. S. *Coord. Chem. Rev.* **2003**, *246*, 103. (b) Lappas, A.; Wills, A. S.; Prassides, K.; Kurmoo, M. *Phys. Rev. B* **2003**, *67*, 144406.

(22) (a) Feyerherm, R.; Loose, A.; Ishida, T.; Nogami, T.; Kreitlow, J.; Baabe, D.; Litterst, F. J.; Süllow, S.; Klauss, H. H.; Doll, K. *Phys. Rev. B* **2004**, *69*, 134427. (b) Nakayama, K.; Ishida, T.; Takayama, R.; Hashizume, D.; Yasui, M.; Iwasaki, F.; Nogami, T. *Chem. Lett.* **1998**, *27*, 497.

(23) (a) Mossin, S.; Weihe, H.; Sørensen, H. O.; Lima, N.; Sessoli, R. *Dalton Trans.* **2004**, 632. (b) Bernot, K.; Luzon, J.; Sessoli, R.; Vindigni, A.; Thion, J.; Richeter, S.; Leclercq, D.; Larionova, J.; van der Lee, A. *J. Am. Chem. Soc.* **2008**, *130*, 1619.

(24) (a) Deakin, L.; Arif, A. M.; Miller, J. S. *Inorg. Chem.* **1999**, *38*, 5072. (b) Kong, D.; Li, Y.; Ross, J. H., Jr.; Clearfield, A. *Chem. Commun.* **2003**, 1720.

(25) (a) Ma, Y.-S.; Song, Y.; Du, W.-X.; Li, Y.-Z.; Zheng, L.-M. *Dalton Trans.* **2006**, 3228. (b) Li, J.-R.; Yu, Q.; Sanudo, E. C.; Tao, Y.; Bu, X.-H. *Chem. Commun.* **2007**, 2602.

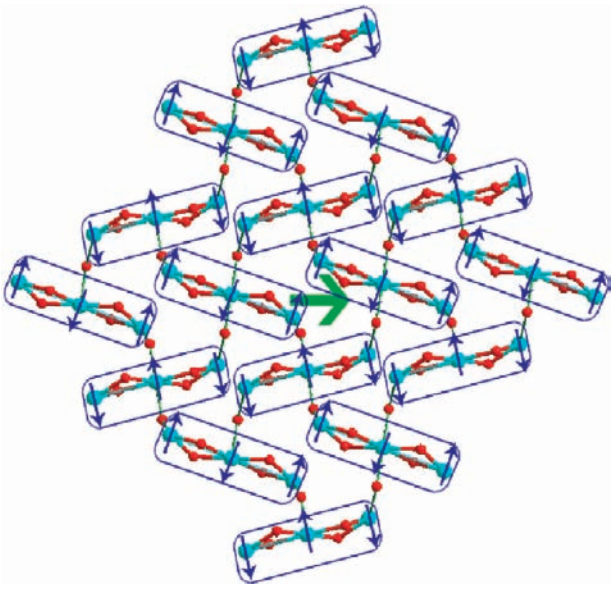

Figure 12. Proposed spin configuration of $Ga_2Cu_3(SeO_3)_6$ (**3**). The blue arrows represent individual moments of Cu^{2+}, and the green arrow represents the net moment. Cu and O atoms are drawn as cyan and red circles, respectively.

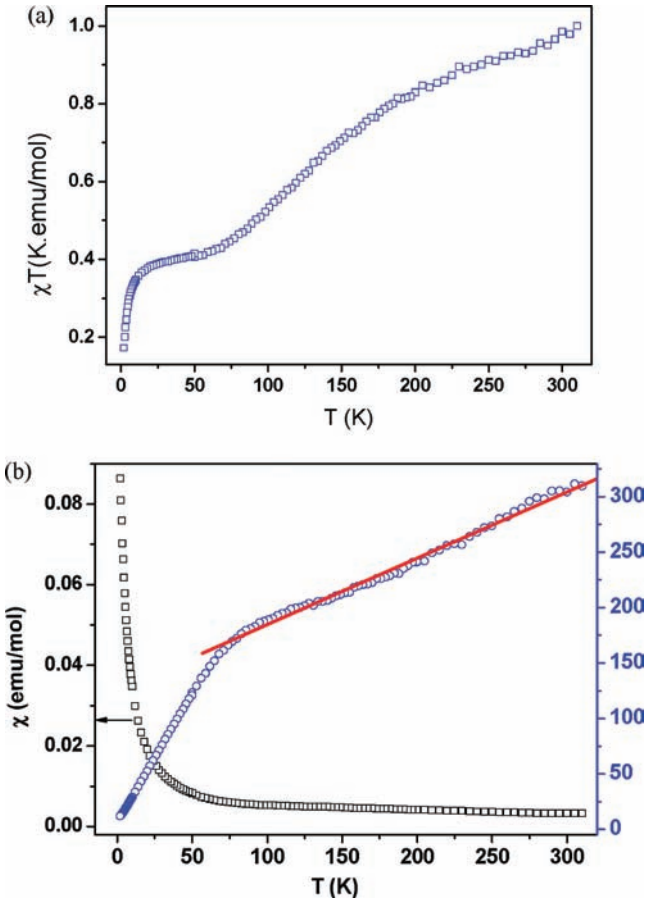

Figure 13. χT vs T plot (a) and the χ and $1/\chi$ vs T plots (b) for $In_2Cu_3(SeO_3)_6$ (**4**). The solid red line represents the fitting according to the Curie−Weiss law.

The χT, χ, and $1/\chi$ vs T plots for $In_2Cu_3(SeO_3)_6$ (**4**) are shown in Figure 13. The value of χT at 300 K is 0.99 emu mol^{-1} K, which is smaller than the expected value for three isolated Cu(II) ions. The continuous decreasing of χT upon cooling indicates predominant antiferromagnetic interactions between the adjacent Cu(II) ions bridged by selenite groups (Cu−O−Cu and Cu−O−Se−O−Cu bridges) within the copper(II) selenite layer (Figure 8b). The temperature dependence of $1/\chi$ between 300 and 80 K approximates Curie−Weiss behavior with $C = 1.7$ emu mol^{-1} K and $\theta = -212.3$ K. The negative sign of the Curie−Weiss constant further confirms the dominant antiferromagnetic interaction between Cu(II) centers. At low temperature χ is independent of the applied magnetic field, indicating that $In_2Cu_3(SeO_3)_6$ (**4**) does not behave as a spin-canted antiferromagnet, which is verified by the ZFC and FC measurements, *ac* susceptibility measurement, and isothermal magnetization (see Supporting Information). The different magnetic behavior for $Ga_2Cu_3(SeO_3)_6$ (**3**) (spin-canted antiferromagnet) and $In_2Cu_3(SeO_3)_6$ (**4**) (antiferromagnet without canting) may be due to the different magnetic superexchange and/or supersuperexchange nets. The indium(III) compounds, with an inversion center between neighboring paramagnetic ions, are not the same as the gallium(III) compound (Figure 14).

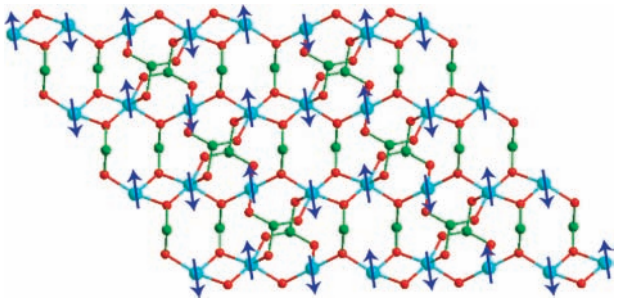

Figure 14. Proposed spin configuration of $In_2Cu_3(SeO_3)_6$ of $Ga_2Cu_3(SeO_3)_6$ (**4**). The blue arrows represent individual moments of Cu^{2+}. Cu, Se, and O atoms are drawn as cyan, green, and red circles, respectively.

Conclusion

In summary, four new copper(II), gallium(III)/indium(III) selenites, namely, $Ga_2Cu(SeO_3)_4$ (**1**), $Ga_2CuO(SeO_3)_3$ (**2**), and $M_2Cu_3(SeO_3)_6$ (M = Ga **3**, In **4**), have been prepared and structurally characterized. They represent the first examples of transition metal gallium(III)/indium(III) selenites. They display three different types of 3D networks and a layered architecture. It was found that the copper source and the reaction temperature have a strong influence on the compositions and structures of the particular metal selenite. In all four compounds, the coordination geometries around Se(IV) cations are similar; however, the selenite anions can adopt various coordination modes with the metal ions. The gallium(III) and copper(II) can exhibit several different coordination geometries, such as GaO_6 octahedron, GaO_4 tetrahedron, and GaO_5 square pyramid for the Ga(III) ion, and CuO_6 octahedron, CuO_5 square pyramid, and CuO_4 square plane for the copper(II) ions. The results of magnetic property measurements indicate that $Ga_2CuO(SeO_3)_3$ (**2**) and $M_2Cu_3(SeO_3)_6$ (M = Ga **3**, In **4**) exhibit strong antiferromagnetic interactions, whereas $Ga_2Cu_3(SeO_3)_6$ (**3**) behaves as a weak ferromagnet below the critical temperature of $T_c = 15$ K. Further studies proved that $Ga_2Cu_3(SeO_3)_6$ (**3**) is a canted antiferromagnet with an estimated large canting

angle of 7.1°. The different magnetic behavior for $M_2Cu_3(SeO_3)_6$ (M = Ga **3**, In **4**) is related to the different magnetic exchange nets. It is expected that the corresponding tellurites will also exhibit novel structures and interesting magnetic properties, and our future research efforts will be devoted to these compounds.

Acknowledgment. This work was supported by National Natural Science Foundation of China (Nos. 20825104, 20731006, and 20821061) and the Knowledge Innovation Program of the Chinese Academy of Sciences.

Supporting Information Available: Details of crystallographic studies (in CIF format), simulated and experimental XRD powder patterns, IR spectra, ZFC and FC measurements, and ac susceptibility measurements for **1**−**4**. This material is available free of charge via the Internet at http://pubs.acs.org.